Epigenomic variation across a polyploid wheat diversity collection

Laura-Jayne Gardiner[1], Ryan Joynson[1], Jimmy Omony[2], Rachel Rusholme-Pilcher[1], Lisa Olohan[3], Daniel Lang[2], Caihong Bai[4], Malcolm Hawkesford[4], David Salt[5], Manuel Spannagl[2], Klaus F. X. Mayer[2,6], John Kenny[3], Michael Bevan[7], Neil Hall[1,8] and Anthony Hall[1,8]

[1] Earlham Institute, Norwich; [2]HelmholtzZentrum München, German Research Center for Environmental Health, Germany; [3]Institute of Integrative Biology, University of Liverpool, UK; [4]Rothamsted Research, UK; [5]University of Nottingham, Sutton Bonington Campus, UK; [6]Wissenschaftszentrum Weihenstephan (WZW), Technical University Munich, Germany; [7]John Innes centre, Norwich; [8]School of Biological Sciences, University of East Anglia, Norwich, UK

Laura-Jayne Gardiner: Laura-Jayne.Gardiner@earlham.ac.uk

Ryan Joynson: Ryan.Joynson@earlham.ac.uk

Jimmy Omony: jimmy.omony@helmholtz-muenchen.de

Rachel Rusholme-Pilcher: Rachel.Rusholme-Pilcher@earlham.ac.uk

Lisa Olohan: L.Olohan@liverpool.ac.uk

Daniel Lang: Daniel.lang@helmholtz-muenchen.de

Caihong Bai: caihong.bai@rothamsted.ac.uk

Malcolm Hawkesford: Malcolm.Hawkesford@rothamsted.ac.uk

David Salt: David.salt@nottingham.ac.uk

Manuel Spannagl: manuel.spannagl@helmholtz-muenchen.de

Klaus Mayer: k.mayer@helmholtz-muenchen.de

John Kenny: J.G.Kenny@liverpool.ac.uk

Michael Bevan: michael.bevan@jic.ac.uk

Neil Hall: Neil.Hall@earlham.ac.uk

Author for correspondence:

Prof. Anthony Hall

Tel: +44 1603 450 989

Email: Anthony.Hall@earlham.ac.uk

Running title: Diversity analysis of SNPs and methylation across wheat varieties

Abstract

Wheat has been domesticated into a large number of agricultural environments and a key question is what drives the ability of crops to rapidly adapt. To address this question, we survey genotype and DNA methylation across a bread wheat landrace collection representing global wheat genetic diversity. We identify independent variation in methylation, genotype and transposon copy number. These three sources of variation all have the potential to contribute to altered gene function and adaptation to different agricultural environments. Methylation and transposon diversity could therefore be used together with sequence polymorphisms in breeding strategies.

Keywords;

DNA methylation, *Triticum aestivum*, Watkins collection, polyploidy, wheat

Background

One of the most important questions in plant breeding is the nature of the genomic variation that has been selected for improving phenotypes. Although it is likely that all forms of genomic change contribute to performance variation and to hybrid vigour, the role of epigenetic variation in crop improvement is not well understood, despite being widespread and highly variable[1]. It is now clear that epigenetic variation can be stably inherited[2,3] and that spontaneous epialleles are rare. Therefore, epigenetic variants could potentially be used in breeding programmes and their contributions to trait variation assessed alongside classical genetic variation. To identify new sources of variation for crop improvement, and to understand the contributions of variation to traits, it is important to assess both genomic and epigenetic variation in crop species.

Epigenetic states of genes in crop plants have been shown to have a major influence on traits. Gene body methylation (gbM) can influence splice-site efficiency by differential CHG methylation of splice acceptor sites, indicating that epiallelic variation can contribute to differential mRNA accumulation[4].

In domesticated polyploid cotton and wild relatives there is extensive epigenetic variation, with methylation differences between homoeologous genes. One example is *COL2D* that is repressed by methylation in wild relatives but is activated by loss of methylation in allotetraploid cotton, influencing flowering time in domesticated lines[5]. The causal gene of a major QTL enhancing resistance to maize stalk rot, *ZmCCT*, is in two epigenetic states. One has CACTA-like TE upstream of *ZmCCT* promoter and one without that has enriched methylated CG that supressed expression and increased disease susceptibility[6]. Similar mechanisms of epigenetic change in gene expression mediated by retrotransposons adjacent to promoters have also been noted in wheat[7]. Tissue-culture induced reduction in methylation of a retrotransposon in the intron of an oil palm *Deficiens* gene alters splicing and causes premature termination[8]. This epigenetic mechanism contributes to the mantled phenotype that limits clonal propagation of this key global crop.

Analyses of DNA methylation patterns in numerous plant accessions and species are starting to reveal the extent of epigenetic variation and the mechanisms involved in generating and maintaining it. Two general patterns of DNA methylation have been identified in plants, transposable element methylation patterns (teM) and gene-body methylation patterns (gbM). In *Arabidopsis thaliana* accessions it was shown that increased gbM is related to constitutive gene expression patterns, and that teM epialleles of genes tend to be expressed at lower levels. Geographic origin was a major predictor of DNA methylation levels and of altered gene expression caused by epialleles[9,10]. It is clear that natural epigenetic variation provides a source of phenotypic diversity alongside genetic variation however, currently, little is known about this epigenetic variation and its interaction with genetic diversity in hexaploid wheat populations.

The genomes of crop plants such as maize and wheat are mainly composed of massive tracts of diverse retroelements and DNA repeats that comprise up to 80% of the genome. These repeats are highly methylated to suppress expression and transposition to maintain genome stability[11]. Wheat is an allopolyploid, comprised of three independently maintained A, B and D sub-genomes that are functionally diploid[12]. Epigenetic mechanisms have been invoked to explain the emergence of key agronomic traits upon formation of hexaploid bread wheat, and to explain alterations in gene expression of homoeologous genes upon polyploidization[13]. Previously we showed that methylation

patterns differ across the A, B and D sub-genomes and in broad terms reflected patterns of methylation of progenitor species[14]. Here we extend our analyses to a core collection of diverse bread wheat landraces in the Watkins collection[15]. Landraces are locally adapted wheat varieties that have not been subject to selective breeding, and represent a pool of diversity reflecting their wide adaptation to different growing environments. Such diversity is beginning to be used in breeding programmes, therefore it is timely to assess and understand both the genomic and epigenomic diversity in this population.

We identified three main sources of variation across wheat landraces; high transposable element (TE) variability, alongside epigenetic and genetic diversity. Although we found a general correlation between methylation patterns and genotypic variation, there was a geographical component to methylation patterns that may indicate a response to or selection by local environmental conditions. We also show that ancestral methylation states may become preferentially 'hard coded' as SNPs via 5-methylcytosine deamination. Finally, we show that tri-genome methylation is the most stable form of methylation, and genome specific methylation patterns correlate with gene expression differences between homoeologous genes.

Results

Methylation and genotype analysis across a wheat landrace diversity panel

To study epigenetic variation across gene-rich regions of the 17 Gb allohexaploid wheat genome, we used genomic enrichment (Agilent SureSelect) followed by bisulfite treatment and Illumina HiSeq paired-end sequencing. Capture probes were designed (12 Mb capture targeting 36 Mb) as described in our previous work[16] (Supplementary Figure 1 from Olohan *et al.*, 2017).

To accurately apply methyl-seq to a diversity panel we require bisulfite treated and untreated sequence data for each wheat accession to identify C-T SNPs, which would otherwise be incorrectly classified as unmethylated cytosines. This was achieved using a modified sequence capture protocol[16,17] that generates two libraries for sequencing from one capture; a bisulfite-treated and an untreated library for each sample. Post-sequencing, the untreated datasets were aligned to the TGAC v1 Chinese Spring

reference sequence and SNP calling was performed (Methods)[18]. We identified 716,018 SNPs on average per sample at ≥5X, of which, 316,767 were homozygous. Homozygous SNPs were used to correct the reference genome for each accession, this corrected reference was implemented for mapping the corresponding bisulfite-treated dataset (Methods).

Bisulfite-treated DNA from single seedlings was examined for 104 core lines from the Watkins landrace collection plus the reference variety Chinese Spring (Supplementary Table 1 and note 1a). We scored methylation at an average of 10.9M cytosines per sample (Supplementary Table 2 and note 1b) and across all samples, on average 98.7% of cytosine bases were successfully bisulfite converted (Supplementary Table 3 and note 1c).

Genetic variation across the Watkins collection clusters geographically

From the 716,018 SNPs that were identified on average per sample, 53,341 SNP sites were identified across the 105 samples where; all samples showed mapping coverage at ≥5X and ≥1 sample had a SNP. For each SNP, the alternate allele frequency per sample was used for hierarchical clustering of the accessions (Methods). Using genotype information for sample clustering, accessions originating from Europe and the Mediterranean tend to cluster together while samples from larger geographic regions in Asia and Russia show higher diversity (Figure 1a and 1b).

The Watkins collection clusters into two main ancestral groups; cluster 1 with 80 accessions (73.8% derived from Europe, Middle Eastern and South Mediterranean/African regions) while cluster 2 has 24 samples (87.5% mainly Asian) (Supplementary Table 4). This genotype-based population structure resembles that from previous analyses of the Watkins collection using array SNP data[15,19] (see Supplementary note 2).

SMPs are variable and cluster geographically across the Watkins collection

Global methylation patterns in Chinese Spring align closely to those of other plant species and previous analyses of Chinese Spring[14,20] (Supplementary note 3; Supplementary Figure 1 and Supplementary Table 5). To assess epigenetic variation across the Watkins collection we identified 853,932 cytosines that were mapped to ≥10X in all 104 samples plus Chinese Spring. 359,500 (42.1%)

of these cytosines were classified as single methylation polymorphism sites (SMPs) between the samples (Supplementary Table 6, Methods). Although methylation variability is high, the SMPs do not preferentially target any of the methylation contexts (CpG, CHG or CHH) (Supplementary Table 6).

0.5% of the 359,500 SMP sites show high methylation conservation between samples (methylated in ≥90%); these were mainly at CpG sites (86.2%) with a bias for transcribed regions (80.2%). Focusing on CpG sites, 13.9% of SMPs were methylated in ≥90 samples highlighting the increased stability of CpG sites compared to non-CpG sites. However, most SMPs (91.5%) are rare variants in <10% of the samples. Unlike highly conserved SMPs, these low-frequency SMPs show less bias for transcribed regions (74.2%) and increased bias for non-CpG sites potentially due to the more dynamic tissue specificity of this methylation (82.5% at CHH sites and 16.4% at CHG sites). Sample-specific SMPs were identified from the 359,500 SMPs (Methods); on average, each sample showed methylation at 26,980 SMP positions with a range of 11,279 to 64,659 SMPs per sample (Supplementary Table 7).

To analyze inter-sample variation in SMPs, for all 359,500 SMP sites, epi-allele frequency per sample was used for hierarchical clustering of accessions for CpG and non-CpG sites individually (Figure 2; Supplementary note 4; Supplementary Figure 2). When we order SMP sites by their total methylation across the accessions (vertical axes, Figure 2); for CpG sites there is a tendency for sites to show extremes of either high or low-level methylation, with typically more methylation in transcribed regions and less methylation in non-transcribed regions. Conversely, non-CpG SMP sites tend to show higher methylation in non-transcribed regions. Clustering the datasets by accession (horizontal axes, Figure 2); inter-sample variation is less obvious for non-CpG sites where most of the methylation is low-level or potentially tissue-specific (Figure 2c). However, more inter-sample methylation variation can be observed at CpG sites with both high and low-level methylation, therefore, accessions can be informatively compared (Figure 2a).

Sample linkage across CpG methylation correlates with geographical sample proximity. Accessions from within the same country of origin tend to show higher linkage and cluster together closely, with 90.3% of the 31 regions analyzed containing a majority of samples (≥50%) from one linkage cluster (Figure 1c and 1d). From the top hierarchical level epigenetic population structure of the Watkins

collection, samples cluster into two groups composed largely of accessions from mixed geographic locations; cluster 1 containing 12 samples derived from 50% Asian and 50% European/Middle Eastern locations and cluster 2 containing 93 samples derived from 41% Asian and 59% European/Middle Eastern locations (Figure 1; Supplementary Table 8). This population structure differs from the genotype-based population structure (Figure 1e); although both split into two sub-populations at the top hierarchical level, for genotype, these sub-populations showed one population from mixed geographic locations while the other was of Asian origin. We statistically compared the two cluster configurations (Figure 1b and 1d); the cluster configuration in the combined SMP and SNP trees (Figure 1e) was non-random (one-sample runs test with 39 runs: Z=-2.53, p = 0.011). This supports the existence of an association between the clustering patterns of SMPs and SNPs.

To determine the similarity of the epigenetic/genotypic profiles, frequency estimates were calculated for SNPs and SMPs across the genome. No correlation between genotype and epi-genotype was detected at this resolution (Supplementary Figure 3). We constructed distance matrices for the 18,965 CpG SMP sites and a comparably sized subset of the 53,341 variable SNP sites. Comparisons were then made using the non-parametric Mantel test to compute Pearson product-moment correlation between the matrices (Methods). A weak positive correlation of 0.394 was observed between the matrices (alpha=0.05, p<0.001) (Supplementary Figure 4). Since this correlation is low, genotype and methylation are likely to be linked but methylation can also develop independently of genetic variation. To corroborate this, we noted a broad-range tendency for samples clustering closely by SMP profile to show similar levels of methylation overall (Figure 2a; Supplementary Figure 5a). However, by ordering samples based on genotypic information and comparing their methylation profiles, only closely related samples share similar methylation levels (Figure 2b; Supplementary Figure 5b).

In summary, the methylation profiles of native accessions for mid/smaller sized countries, e.g. the UK, Greece, Afghanistan, Cyprus and Italy, are more likely to cluster together. These lines most likely evolved in similar environmental conditions and have similarly adapted methylation profiles. Conversely, we see samples from geographically distant locations with comparable methylation, this may represent conserved environmental conditions that have resulted in a similar adaptive change in methylation profiles. For samples where we have more accurate positional information for

geographical origin, this association between methylation and local adaptation is clearer (see Supplementary Table 9; Supplementary note 5).

Distinctive patterns of methylation are associated with different classes of gene function.

Our analysis of the landraces clustered accessions with similar patterns of methylation into 8 distinct groups (Figure 1d). To assess if these clusters represented any functional consequences of gene methylation, genes that were methylated within each cluster were analysed by GO enrichment for molecular functions (topGO, $p < 0.05$). At this level of analysis, all 8 clusters had distinctive profiles of enriched GO terms across multiple functional categories of genes (Supplementary Table 10 and 11). To ascertain if there were any functional consequences of gene methylation patterns within these clusters, information on differential gene expression were included in these analyses, and are shown later in Supplementary Tables 24-26.

Tri-genome is the most stable form of methylation

We classified methylation as tri-genome (in three sub-genomes), bi-genome and uni-genome (in two or one sub-genome respectively) (Methods, Supplementary Table 12). Supplementary Table 13 details differentially and tri-genome methylated CpG, CHH or CHG sites averaged across the samples. The observed methylation landscape largely reflects that seen in our previous analysis (Supplementary note 6)[14].

To assess the relative stability of uni-, bi- and tri-genome methylation across the Watkins collection we identified positions that were uni-, bi- or tri-genome methylated in one or more of the samples. From these positions, we selected all sites that had mapping coverage ≥10X in all accessions, independent of their methylation status. Figure 3a highlights a median of 20.95% of accessions showing conserved tri-genome methylation compared to only 2.85% of accessions with conserved uni- or bi-genome methylation. Furthermore, 14.3% of tri-genome sites were methylated in the majority of samples (>= 90%) whereas, on average, only 1.08% of uni- and bi-genome sites showed methylation conservation on this scale (Supplementary Table 14). Tri-genome methylation is significantly more conserved across the accessions compared to uni and bi-genome methylation respectively (bi genome t=74.66, df=16508, p-value <2.2e-16; uni-genome t=67.56, df=17848, p-value <2.2e-16) and this tri-

genome methylation is evenly distributed across the genome (Methods, Supplementary Figure 6; track 1, 5 and 9). Gene Ontology enrichments, for genes associated with the most stable subset of tri-genome methylation (in >= 90% of samples), included core biological activities within the plant such as phosphorylation, intracellular transport, transcription regulation, oxidation-reduction, proteolysis and methylation (Supplementary Table 15).

Genome-specific methylation associates with homoeologous SNPs

We analyzed methylation variation where all samples contained the same sequence. Looking at the cytosine residue sites that were mapped to ≥10X in all of the samples, most (89.0%) shared the same genetic sequence, i.e. cytosine CpG/CHG/CHH context, and were, therefore used to identify 359,500 SMPs. Methylation is a source of variation in the absence of genetic variation; however, we also assessed the impact of SNPs on methylation. Across all the samples, at cytosine sites showing tri-genome methylation, the average percentage of sites where a SNP altered the cytosine context between the sub-genomes of wheat is unsuprisingly low (3.50%)-methylation levels at these positions are conserved between the genomes. Conversely, at uni-genome methylation sites, it is more common to see a homoeologous SNP between the sub-genomes of wheat that differentiates the methylated genome from the other two sub-genomes (at 65.1% of uni-genome methylated sites). This SNP typically infers a CpG site from a non-CpG site (96% of the time).

Ancestral methylation can be hard-coded as SNPs

We generated genotype and methylation information for the sub-genome D ancestor (*Ae. tauschii*) to allow comparison with Watkins accessions. We observe that ancestral methylation significantly increases the chance of encountering a different allele in hexaploid bread wheat by ~4-fold (t=-30.42, df=103, p-value<2.2e-16). It shows a predominance for C-to-T/G-to-A transitions that is also statistically significant (t=-283.7129, df=103, p-value<2.2e-16) (Supplementary note 7a, Figure 3b and 3c). These C-to-T/G-to-A transitions are characteristic of the deamination of a methylated cytosine. This apparent preferential deamination of 5-methylcytosine to thymine, has been observed in other organisms[21] and in *Arabidopsis* where is contributed to bias in spontaneous nucleotide mutation[22]. Furthermore, there was high methylation stability in wheat where most methylation was conserved

between *Ae*. *tauschii* and sub-genome D (83.7%). There was a low level of methylation gain in sub-genome D compared to *Ae*. *tauschii* (3.1%) (Supplementary note 7b).

Differentially methylated region (DMR) profiles reflect SMP profiles

Gene expression changes are often associated with methylated regions rather than single methylated nucleotides. Using non-overlapping 100bp windows across the genome, DMRs were identified in the CpG, CHG and CHH contexts between each sample and Chinese Spring (Methods)[23]. Per sample, on average 58.7 CpG (range 37-89), 13.4 CHG (range 8-23) and 20.1 CHH DMRs (range 0-168) were identified (Supplementary Table 16). In total 2,356 DMR regions of 100bp were identified across the samples compared to Chinese Spring (491 CpG, 96 CHG and 1,769 CHH DMRs). 1,901 of these DMRs associated with 1,744 genes and 71 DMRs were located in promoter regions associated with 64 genes. For all 2,356 DMR sites, similarly to the analysis for SMP sites, the percentage difference in methylation per sample compared to Chinese Spring was used to cluster the accessions (Supplementary Figure 7). A strong positive correlation exists between the clustering of CpG SMPs and DMRs and as such similar trends are observed with DMRs as was seen for SMPs (Supplementary note 8).

For all accessions, we summarized the number of differentially methylated genes (DMGs) by methylation context i.e. genes with a DMR compared to our reference Chinese Spring (Supplementary Figure 8a). Variation between accessions was highest for CHH DMGs, while the number of genes showing differential methylation in the CpG and CHG contexts is more stable across accessions. CHH variability may reflect the reported dynamic nature of CHH methylation during plant development[24]. There was no evidence of bias in the methylation contexts CpG/CHG/CHH between the wheat A, B and D sub-genomes (supplementary figure 8b-d, and 9a-c).

Samples cluster by preferentially targeted genes and gene families (Supplementary note 9)

Accessions were clustered based on similarities in the proportion of the number of genes that are methylated in each gene family (vertical dendrogram, Figure 3d). We observe inter-accession variation in gene families highly targeted for methylation. However, a number of gene families are preferentially targeted for methylation across multiple accessions with a high proportion of genes in the family

methylated (horizontal dendrogram Figure 3d, coloured red in heatmap). GO enrichment analysis revealed the most common molecular functions associated with highly methylated gene families within and between accessions (Supplementary Tables 17 and 18). Hexokinase activity and glucose binding were the top enriched molecular functions for highly methylated gene families conserved between samples (Supplementary Table 18). These terms are linked to cellular glucose homeostasis and support the hypothesis that some gene families are consistently targeted by methylation across the Watkins collection.

We performed GO enrichment analyses on gene families that were less targeted by methylation within and between accessions (Supplementary Table 19 and 20). NAD binding and N-methyltransferase activity were the top enriched molecular functions for low-level methylated gene families conserved between samples (Supplementary Table 20). Enriched GO terms for highly methylated gene families and less methylated families did not overlap, suggesting that genes of the same molecular function are either consistently methylated or non-methylated across the accessions.

Finally, we focused on CpG methylated genes, appearing in a high, medium or low number of accessions (Methods). Supplementary Figure 10 shows the distribution of the number of genes in the 3 groups: high, medium and low; ~35% of the 2145 CpG methylated genes were present in ≥90 accessions. Previously, we observed that few (0.5%) SMPs were methylated in at least 90% of the samples but this analysis considered CpG and non-CpG sites. For CpG sites, 13.9% of SMPs were methylated in ≥90 samples. Therefore, at the gene level, we see a ~2.5-fold increase in methylation conservation across accessions compared to SMPs (13.9% to 35%). This demonstrates an increased tendency for methylation targeting the same genes across accessions even if the specific cytosine sites differ. Furthermore, the enriched molecular functions within the high, medium and low groups were different with no overlaps (Supplementary Table 21).

Differential methylation correlates with changes in gene expression

To test the correlation between methylation and gene expression across the Watkins collection, we performed RNA-seq analysis, using 14-day-old wheat seedlings on 12 samples in triplicate, which represent phenotypic tails for; height, heading date, thousand-grain weight and grain width

(Supplementary Table 22). We generated gene expression level estimates to allow pairwise comparisons and identify differential gene expression between the samples (Methods). 105,425 wheat genes were analyzed across the sample-set and comparing the 12 samples, 16,112 were differentially expressed; 32.3% from the A-genome, 44.6% from the B-genome and 23.1% from the D-genome (15.3% of analyzed regions) (p-value <0.05).

We normalized allelic gene expression so that per site cumulative expression values for the A, B and D sub-genomes were equal to 100%. The average expression level of sub-genome A across the 289 tri-genome sites associated with promoter regions was 34.22%, sub-genome B 33.43% and sub-genome D 32.35%-demonstrating approximately balanced allelic expression in the sub-genomes. The average expression level of the methylated genome across the 128-promoter associated uni-genome methylation sites was 28.82% while that of the other genomes was on average 35.59%. Therefore, there was a decreased expression of the promoter-methylated sub-genome in comparison to the other two sub-genomes ($p<0.0001$, $t=5.95$, $df=254$).

Previously, we identified DMRs across the samples by comparing non-overlapping 100bp windows with Chinese Spring (Methods). Here, we focused on the 12 samples that were analyzed by RNA-seq and implemented pairwise comparisons to identify DMRs to allow correlation with differential gene expression from the same pairwise comparison. Inter-sample pairwise comparisons yielded an average of; 58.9 CpG, 11.2 CHG and 30.0 CHH DMRs per comparison (Supplementary Table 23). 32.3% of the DMR's were associated with differentially expressed genes. This reflects a more than 2-fold enrichment in the proportion of genes overall that show differential gene expression. All differentially expressed genes that correlated with DMRs were subjected to the enrichment of molecular functions and biological processes using topGO ($p < 0.05$) (Supplementary Tables 24, 25 and 26). DMRs that correlate with differential gene expression are more likely to be influencing this expression change and here, CpG DMRs show enrichment for biological processes related to homoeostasis and essential housekeeping. Conversely, non-CpG methylation associates with differentially expressed genes in biological processes related to stimuli response.

For genes that were both differentially expressed and methylated, there is also a bias for enriched GO terms with molecular functions relating to metal ion transportation (Supplementary Table 24). Enrichment for transporter and metal ion binding activity and was seen across SMP sample clusters (Supplementary Table 10 and 11, Figure 1d). This bias of methylation to affect gene expression in pathways related to detoxification and metal ion transportation could be an adaptive response to differences in the soil composition in the country of origin of the sample (Supplementary Table 25, Supplementary note 10). Furthermore, the methylation and gene expression correlations fit the directionality models predicted by previous studies for methylation based on genic positon[25,26,27]. We focused on genes showing differential expression and methylation that had a clearly defined metal ion interaction. This narrowed our analysis to; firstly, a Sodium/hydrogen exchanger that showed up-regulated expression from a (former) Yugoslavian accession 1190352 compared to the Cypriot accession 1190292. Up-regulation of this exchanger is associated with adaptation to salt tolerance that is biologically relevant since Yugoslavia reportedly had large areas of salt-affected soils when Cyprus was at the time unaffected[28,29]. Furthermore, leaves from the Yugoslavian accession 1190352 show significantly higher Na concentrations (average 2182.1 ppm) compared to accession 1190292 (average 1257.7 ppm) (t=5.013, df=4, p-value=0.0074, Supplementary Figure 11a, Methods). Secondly, the ATP-dependent zinc metalloprotease *FTSH 2* showed up-regulation in the Palestinian accession 1190398 compared to a number of other accessions. *FTSH* is down-regulated after exposure of plants to elevated zinc concentrations[30]. Here, the Palestinian accession 1190398 shows *FTSH 2* up-regulation coupled with a lower average leaf Zn concentration (48.63 ppm) compared to each of the three accessions 1190141-China (66.64 ppm), 1190292-Cyprus (68.55 ppm) and 1190352-Yugoslavia (75.28 ppm) for which leaf Zn concentrations were available. The differences in zinc concentrations were not significant however; they fit the directional model for zinc response (t=1.105, df=10, p=0.2949, Supplementary Figure 11b, Methods).

Early heading date associates with SMP but not SNP profiles

The average expression levels per sample (across the replicates) for the 16,112 differentially expressed genes in one or more of the pairwise sample comparisons, were used for hierarchical clustering (Figure 3e). The barcodes in Figure 3e allow comparison of gene expression clusters with SNP/SMP clusters from Figure 1b and 1d, respectively. Samples that cluster into the same clades by gene expression

profiles also cluster closely by SNP profile. This is demonstrated in Figure 3e by conserved colour blocks in the SNP barcode within dendrogram clades. Conversely, samples with divergent expression profiles typically belong to different SNP dendrogram clades. These patterns are also apparent from correlating gene expression and SMP profiles.

Heading date associates with a distinct clustering of samples (Figure 3e). The two samples 1190209/1190034, with earlier heading dates, show the most similar gene expression profiles of all analyzed samples. The samples 1190481/1190181, with later heading dates, cluster together almost as closely but importantly, they are segregated from 1190209/1190034. The two samples with earlier heading dates cluster into the same SMP clade but different SNP clades while, conversely, the samples with later heading dates cluster into the same SNP clade but different SMP clades. This could indicate a common role for methylation in the establishment of an early heading date that correlates with gene expression profile.

We identified differentially expressed genes between early and late heading samples in a pairwise comparison matrix if they were conserved across all replicates; 46 annotated genes were identified (Supplementary Table 27). This includes genes previously linked to flowering time or heading date regulation e.g. REVEILLE 8-like/LHY-CCA1-like 5 that is here down-regulated in early heading date plants[31]. Where methylation associates with these genes, it correlates with the expected directional effect (Supplementary note 11a). Furthermore, Supplementary Table 28 shows the most significantly enriched GO terms and associated biological processes respectively for the 46 differentially expressed genes (topGO, $p < 0.05$). Enriched processes are predominantly related to meristem growth, development and cell cycle process and phase transition and therefore show biological relevance to the phenotype (Supplementary note 11b).

Transposable element (TE) abundance is highly variable across the Watkins collection

Analysis of Chinese Spring off-target sequence data demonstrates that it is unbiased sampling of the genome, equivalent to low coverage shotgun sequencing of total wheat DNA, since proportions of TE types closely match those seen in previous shotgun sequence data (Supplementary Table 29, Supplementary note 12a)[32]. To assess TE methylation levels for each Watkins accession, off-target

sequencing data was aligned to the wheat TREP database of repeat sequences[33]. Across the Watkins collection, transposons are highly methylated compared to the enriched gene-rich regions (Supplementary note 12b, Supplementary Table 30). This hyper-methylation of repeats is consistent with other plant species and is associated with reducing transposon mobilization.

We observed high variability across the Watkins collection in the proportions of reads aligning to each TE compared to Chinese Spring (Methods, Supplementary note 12c, Figure 4); expansion of retrotransposons is most frequent with 44.2% of accessions showing an increase in mapped base-space of 2% or more compared to Chinese Spring although, large expansions of the mapped base space of 8-10% are seen in DNA transposons in a small subset of lines (Figure 4a). TE expansions do not correlate closely with gene-associated SNP/SMP clusters or geographical clustering. It appears that expansion within the TIR; CACTA group are responsible for increasing the proportion of DNA transposons compared to Chinese Spring in a subset of Watkins accessions (Figure 4b). This expanded group of DNA transposons showed conservation of the high methylation levels seen typically across TEs (Figure 4i). SINE and LTR; Gypsy retrotransposons show prominent and variable expansion compared to Chinese Spring across the Watkins collection (Figure 4c) coupled with conservation of the high methylation levels seen typically across TEs (Figure 4g and 4h). These findings are consistent with previous observations that LTR retrotransposons are epigenetically controlled and a major contributor to genome size change in plants[34].

Conclusions

Using sodium bisulfite treatment and targeted gene enrichment, we observe high epigenomic diversity in the Watkins collection; we demonstrate that methylation is a standalone source of variation in the absence of genetic variation, however, if two wheat accessions show more closely related genotypes then their methylomes are more likely to be related. Both methylation and genotype are influenced by the geographical origin of the sample, although genotypic profiles cluster across wider geographic regions while the methylation profiles of accessions tend to cluster into more local groups. Therefore, we hypothesize that methylation acts as a fast-adaptive response to environmental stimulus.

Furthermore, we show that ancestral methylation increases the chance of C-to-T or G-to-A transitions in Chinese Spring wheat that are characteristic of the deamination of a methylated cytosine and may demonstrate this transfer of methylation to SNPs[21,22]. This phenomena could be an important driver of evolutionary change.

We show that tri-genome methylation is more conserved between accessions and therefore the most stable form of methylation, while genome specific methylation sites show enrichment for homoeologous SNPs that differentiate the genome that is methylated from the other sub-genomes. This SNP typically infers a CpG site from a non-CpG site. Tri-genome methylation, correlates with equal expression levels across the 3 sub-genomes while uni-genome methylation correlated with a significant reduction in expression of the affected sub-genome compared to the other two sub-genomes in promoter regions.

Watkins accessions were clustered according to methylation profiles and the clusters show unique profiles of enriched gene function, these variations could contribute to the underlying phenotypic differences between the accessions. Using gene expression analyses, we saw conserved methylation and gene expression profiles in accessions with an early heading date, suggesting that methylation may play a role in the co-ordination of heading date in wheat. DMRs linked directly to gene expression show a bias for genes related to metal ion transportation that links to phenotypic change and could be part of an adaptive response that has been maintained in certain accessions due to differences in the soil composition in the country of origin of the sample.

In addition to epigenomic diversity across the Watkins collection, using Chinese Spring as a baseline, we observe the potential expansion of retrotransposons SINE and LTR; Gypsy most frequently, although some of the largest expansions are seen in a small subset of lines in DNA transposons. These expanded groups of TEs showed conservation of the high methylation levels seen across TEs.

We explore genome-wide epigenetic, alongside genotypic and TE variation across a diverse landrace cultivar collection and open up a new level of genetic variation, which can be exploited by breeders. This provides further opportunities to address important biological questions such as the interaction

between epi-type and genotype, the role of epigenetics in the domestication of crops and the stability of and long-term function of methylation in a polyploid genome.

Figure legends

Figure 1. Geographical sample origins combined with hierarchical cluster analysis on 104 samples from the Watkins core collection plus Chinese Spring wheat. (a) Geographical positions of the samples colour coded by their allocated cluster from **(b)** after SNP hierarchical clustering**. (b)** Dendrogram constructed using the complete linkage method within the R package hclust to cluster samples based on SNP allele frequency across 53,341 SNP sites. The tree was cut into 8 groups (excluding the reference Chinese Spring) using the R package cutree and these clusters are colour-coded (Methods). **(c)** Geographical positions of the samples colour coded by their allocated cluster from **(d)** after CpG SMP hierarchical clustering**. (d)** Dendrogram constructed using the complete linkage method within the R package hclust to cluster samples based on methylation levels across 18,965 CpG SMP sites (taken from the 359,500 SMPs that were identified within the sample set). The tree was cut into 8 groups using the R package cutree and these clusters are colour-coded (Methods). **(e)** SNP based-dendrogram from **(b)** with individual samples colour-coded as per their cluster from the SMP-based dendrogram from **(d).** For geographical sample positions in **(a)** and **(c)** squares outlined in black represent samples with detailed positional information that is used for plotting, squares with no outline represent samples with only a country of origin. AU p-values were computed for the main clusters in **(b)** and **(d)** using the R package pvclust and are shown in red (Methods).

Figure 2. Visualizing methylation levels for the 105 wheat samples across 359,500 SMP sites. Using sites with coverage in all 104 Watkins collection accessions plus Chinese Spring we generated heatmaps for methylation levels across **(a)** CpG-SMPs **(b)** CpG-SMPs with accessions ordered by genotype using the heatmap from **(a)** with accessions re-ordered based on figure 1b's SNP clustering dendrogram (shown on top horizontal axis) and **(c)** Non-CpG SMPs. Rows correspond to individual SMP sites and columns indicate accessions. The coloured row labels (barcodes) on the left of the heatmap indicate which genomic location a SMP falls into (see legend). SMP sites are ordered by their

total methylation across the accessions on the vertical axes and accessions are clustered by SMP profiles on the horizontal axis (Methods).

Figure 3. Analyzing methylation profiles across the Watkins collection. (a) Violin plots show the percentage of accessions showing methylation per analyzed site. Analyzed sites include Tri-genome, Bi-genome and Uni-genome methylated sites. A comparative subset of 11,769 sites was used for each category. **(b)** Ancestral methylation associates with an increased SNP rate**.** The percentage of methylated versus non-methylated *Ae. tauschii* cytosines that show a different allele in the Watkins. **(c)** Ancestral methylation demonstrates that 5-methylcytosines are preferentially deaminated to thymine. The percentage of methylated versus non-methylated *Ae. tauschii* cytosines with a C-to-T/G-to-A transition across the Watkins collection. **(d)** Sample clustering based on the gene families targeted by methylation. Many accessions from the same geographical origin show the same gene families targeted by methylation; thus, clustered close to each other in the Accessions axis (vertical dendrogram). Alongside the vertical dendrogram the two columns of row barcodes (left and right) correspond to the SMP clusters in Figure 1d and SNP clusters in Figure 1b respectively. **(e)** Sample clustering of the 12 accessions subjected to RNA-seq using average gene expression across the replicates for genes showing differential expression between at least 2 lines (after log2 transformation). Below the horizontal dendrogram the two barcode rows (top and bottom) correspond to the SMP and SNP clusters in Figure 1d and 1b respectively. Accessions are labelled by line number, country of origin and phenotype i.e. TGW (thousand grain weight), HD (heading date), GW (grain width) or Height with maximum values in green and minimum values in red.

Figure 4. Analyzing transposable element methylation profiles across the Watkins collection. (a) Base-space per Watkins accession aligned to DNA-transposons and retrotransposons in comparison to Chinese Spring (Methods) **(b)** Base-space per Watkins accession aligned to DNA-transposons in comparison to Chinese Spring. **(c)** Base-space per Watkins accession aligned to retrotransposons in comparison to Chinese Spring. **(d)** Base-space per Watkins accession aligned to retrotransposon-SINE in comparison to Chinese Spring plotted versus the total cumulative percentages of enriched cytosine residues (gene-associated) that were methylated for CpG, CHG and CHH methylation. **(e)** as per **(d)** but for retrotransposon-LTR, Gypsy **(f)** as per **(d)** but for DNA-transposon-TIR, CACTA **(g)** Base-space per Watkins accession aligned to retrotransposon-SINE in comparison to Chinese Spring plotted versus the total cumulative percentages of TE-associated cytosine residues that were methylated for

CpG, CHG and CHH methylation. **(h)** as per **(g)** but for retrotransposon-LTR, Gypsy **(i)** as per **(g)** but for DNA-transposon-TIR, CACTA.

Methods

Design of the methylation enrichment system. The 12Mb target sequence for this Agilent enrichment system was generated as per Supplementary Figure 1 from Olohan *at al.*[16]. 99,949 120-mer RNA baits were designed for the capture. The 120-mer baits were uploaded onto Agilent's EArray (online custom microarray design tool) to allow submission for manufacture. Bait 'boosting' was selected to allow excess unused design space (less than 1Mb in this case) to be filled with repeat sequences of baits that are predicted to perform less efficiently i.e. those with an above average GC content are 'boosted' to ultimately gain even depth of sequence coverage across the target region.

Preparation and mapping analysis of DNA samples. Single seedlings were examined for all 104 core lines from the A. E. Watkins bread wheat landrace collection plus the reference variety Chinese Spring (Supplementary Table 1). Total genomic DNA was extracted from the areal tissue of these 14-day-old wheat seedlings grown at a constant 24°C under long days using Qiagen DNeasy plant mini kits. 3μg of each sample was sheared for 22 cycles of 30s on, 30s off, using a Bioruptor Pico (Diagenode) and 0.65ml Bioruptor tubes. Fragmented DNA was purified using 1.8 × Agencourt AMPure XP beads (Beckman Coulter) and then used as input material for preparation of libraries according to Agilent's SureSelect^{XT} Methyl-Seq Protocol Version C.0, January 2015. The pre-capture libraries were quantified by Qubit double-stranded DNA high sensitivity assay (Thermo Fisher Scientific) and the size distribution assessed by analysis on a Fragment Analyser (Advanced Analytical Technologies) using a high sensitivity NGS Kit. Each library was then enriched using the 12 Mb custom SureSelect RNA oligomer baits with use of a modified sequence capture protocol to allow genetic and methylation analysis of the same enriched genomic DNA sample by splitting the sample post-capture[16]. For this, hybridization set-up and post-capture washing were carried out in batches of 48 using a Tecan Freedom EVO NGS Workstation. Enriched DNA was eluted from the Streptavidin beads with 27μl of Elution Solution and then neutralised with an equal volume of Neutralisation Solution prior to purification using 1.8 × Agencourt AMPure XP beads. At this point

the enriched purified DNA was divided at a ratio of approximately 3:1. ¾ of the DNA was bisulfite treated using a Zymo Research EZ-96 DNA Methylation Gold Kit (deep well format) according to the manufacturer's instructions, but with double elution from the Binding plate using 16µl of M-Elution Buffer each time. The bisulfite-converted DNA and the remaining ¼ of untreated enriched DNA were amplified in parallel as described by Olohan *et al.,* 2017[16] but using 10 PCR cycles for the final indexing amplification. Following purification and QC, final libraries were pooled in equimolar amounts (genetic and methylation analysis) and sequencing was carried out on an Illumina HiSeq 4000, with version 1 chemistry, generating 2 x 150bp paired-end reads.

The non-bisulfite treated paired-end sequencing datasets for the samples were mapped to the TGAC reference sequence using BWA MEM version 0.7.10[35]. Mapping results were processed using SAMtools[36]; any non-uniquely mapping reads, unmapped reads, poor quality reads and duplicate reads were removed. SNP calling was carried out using the GATK[37] Unified genotyper (after Indel realignment), which was used with a minimum quality of 30 and filtered using standard GATK recommended parameters, a minimum coverage of 5 and homozygous SNPs only selected (alternate allele in ≥80% of sequencing reads). Homozygous SNP alleles were used to correct the TGAC reference sequence to generate an accession specific reference sequence for each analyzed accession that was implemented for mapping the corresponding bisulfite-treated dataset to using Bismark, an aligner and methylation caller designed specifically for bisulfite-treated sequence data[38].

For mapping analyses using Bismark the non-directional nature of the library was specified and subsequently SAMtools was used to identify and remove duplicate reads. The Bismark methylation extractor tool was used to identify all cytosine residues within the mapping and categorize the reads mapping to them as un-methylated or methylated at that position while also detailing which type of potential methylation site was present (CHH, CHG or CpG). This output can then be used to calculate the percentage of the reads that were methylated at each cytosine residue site. Under the same rationale differential methylation was identified between sub-genomes and/or samples at a minimum difference of 50% to ensure elimination of replicate variance and the analysis of genuine methylation changes.

Alignment of the three sub-genomes of wheat. The three sub-genomes were aligned using the software NUCmer from the MUMmer package that is specialized for the alignment of incomplete genomes with large numbers of reference contigs[39]. After the alignment, using the MUMmer package,

result files were filtered to determine a one-to-one mapping of sub-genome A to B and A to D and indels were identified between the sequences. Finally, for each sub-genome A cytosine/guanine position in the TGAC reference sequence, if this was in a region showing an alignment with both sub-genome B and sub-genome D, the corresponding position in sub-genomes B and D was calculated. Indel information was used to ensure that single positions were correctly translated between aligned sub-genomes even if alignments contained gaps.

Calculation of bisulfite conversion rate. Bisulfite conversion rates can be measured by mapping reads to the chloroplast genome, which is un-methylated[40,41]. While we did not enrich for chloroplast DNA, because we used total wheat DNA, a proportion of our off-target sequences mapped to the wheat chloroplast genome. The off-target DNA was mapped to an average of 66.5% of the chloroplast genome across all samples to 406X per sample (Supplementary Table 3).

Setting thresholds for calling methylation

To discriminate methylated CpG, CHG and CHH sites from non-methylated residues we used standard thresholds for each category based on previously published methodologies[14] that take into account the tendency for a high-level average CpG methylation and low-level average non-CpG methylation in gene-rich enriched datasets that was reflected in this study (Supplementary Figure 1). Thresholds of ≥75% methylation were used to categorize the CpG data as methylated and thresholds of ≥10% methylation to categorize the CHG and CHH sites as methylated. However, this means that intermediate-level methylation, which is likely to be associated with tissue specific regulation, was not fully described and is beyond the scope of this study.

Implementation of Methylkit[42]. The software Methylkit was implemented to identify regions of differential methylation using positional information for each cytosine plus the number of reads hitting it per sub-genome and each read's methylation status. Pairwise comparisons were used and as such the Fishers exact test was used to discriminate statistically significant differences ($q<0.01$ and methylation difference of ≥50%). Firstly, Methylkit was implemented to define differential methylation between the sub-genomes of wheat, within each sample, in regions where the three sub-genomes could be aligned. Differences were recorded at single cytosine residues between one genome and the other two (uni-genome methylation) and vice versa (bi-genome methylation). Finally, after identification of DMRs, Methylkit was implemented with pairwise comparisons of samples to define DMRs between the two samples ($q<0.01$ and methylation difference of ≥50%).

Identification of SMPs and SNPs. SMPs were identified by looking for sites that were covered by at least ten reads and were either called methylated (denoted as 100%) using our standard thresholds, or showed no methylation (< 1%), which we defined as an un-methylated site (denoted as 0%). Any other sites with no coverage were listed as missing or with intermediate methylation levels were listed as heterozygous (denoted as 50%). A general SMP was defined as any site with sufficient coverage for all of the analyzed samples where; at least two accessions were called methylated, at least two accessions were called un-methylated and where all samples contained the same sequence as the Chinese Spring reference genome i.e. no SNP altering the cytosine context between CpG, CHH and CHG. An individual sample SMP was defined as any site from the general SMP list where the sample was denoted as being 100% methylated. SNPs were called as previously detailed. For clustering analyses 53,341 SNP sites were identified across the 105 samples where; all samples showed mapping coverage at ≥5X and ≥1 sample was found to have a SNP i.e. variable sites.

Dendrogram construction. Throughout this study, dendrograms are used to present clustering results. If these dendrograms accompany heatmaps then they have been produced using the R function heatmap.2 from the gplots package with the default clustering parameters (complete linkage method with Euclidean distance measure). The dendrograms that lack heatmaps were produced by first generating a distance matrix with R's dist function and passing this matrix to the hclust function, both with their default parameters. Furthermore, the R package pvclust was implemented to generate the dendrograms as detailed however with the additional computation of p-values for clusters; AU (Approximately Unbiased) p-values were computed by multiscale bootstrap resampling (minimum bootstrap number of 10,000).

The SNP based tree (figure 1b) was cut into 9 groups using the R package cutree. The first group, consisting of Chinese Spring only is a result of this accession being used as the reference genome and as such was disregarded from the analysis. The remaining 8 clusters represent, moving down the dendrogram, the lowest cut where we can maximize group number for analysis but the majority of groups still include enough samples to be informative with AU p-values ≥70% i.e. lowest cut where at that point and above >50% of cluster groups show >5 members. The SMP based tree was similarly cut into the 8 main groups to allow direct comparison of SMP and SNP groups.

Distance matrix construction and comparison. Distance matrices were constructed individually for the 18,965 CpG SMP sites and a subset of 17,780 of the 53,341 variable SNP sites using the R

function dist. These distance matrices were then compared using the mantel.randtest function in R to perform the Mantel test with 999 permutations. Distance matrices were also converted to heat maps using the R function heatmap.2 without dendrogram construction or clustering.

Construction of pseudo chromosomes. We used 21 wheat chromosomal pseudomolecules that were created by organizing and concatenating the TGAC genome assemblies onto POPSEQ-based pseudomolecules using the software NUCmer[39,43,44]. After the alignment, using the MUMmer package, result files were filtered to determine a one-to-one mapping of TGAC sub-genome A to POPSEQ-based sub-genome A, B to B and D to D. Relative positions for the TGAC contigs along the POPSEQ chromosomal pseudomolecules could then be used to order them into our chromosomal pseudomolecules.

Identification of DMRs. We focused on the 853,932 cytosine residue sites that were mapped to a minimum of 10X in all of the 104 samples plus Chinese Spring. Using these sites, DNA methylation for the three contexts (CpG/CHG/CHH) was averaged independently across non-overlapping 100bp windows. A window was only considered if a minimum of 5 cytosines were included in the region. This yielded 2,277 CpG, 3,721, CHG and 44,371 CHH windows for analysis. For every window, each sample was compared individually with Chinese Spring (see implementation of Methylkit) to identify DMRs. For CpG and CHG sites a DMR was called if a region showed a difference in methylation of at least 50% (q-value < 0.01), however, for CHH sites a DMR was called if a difference of at least 15% was observed (with one sample showing 'low' or ≤5% methylation and a q-value of < 0.01).

Association between SMP and SNP clusters, and enrichment for molecular functions. Gene set enrichment analysis (GSEA) was performed on the 8 main SMP clusters that are shown in (Figure 1d) using the R package topGO[45]. The gene sets in each of these clusters were collated from all samples within each cluster and enriched for molecular functions using gene ontology, GO. TopGO integrates the GO topology in the scores and identifies over-represented terms globally. For the enrichment analysis, we used genes from CpG DMRs in the 104 samples referenced to Chinese Spring (with an absolute methylation difference of ≥50% and a minimum of 5 cytosines).

The arrangement of accessions in the merged SMP (Figure 1d) and SNP (Figure 1b) trees in Figure 1e were assessed for randomness. The randomness test evaluates the association between the methylation (SMPs) and genetic (SNPs) components. We used the non-parametric one-sample runs test[46] to assess the randomness of accession membership in the coloured clusters (Figure 1e). By maintaining the

ordering of samples in the SNP dendrogram (Figure 1e), the 8 SMP clusters shown in distinct colours were assigned to different categories and the neighbouring accessions in the tree were indexed as dichotomous variables (1 for the same cluster membership, and 0 otherwise). The two classes had large samples with 61 (ones) and 43 (zeros); thereby, justifying the large-sample test approximation to the standard normal distribution, $N(0,1)$.

Enrichment analysis for the methylated genes, in 3 groups (high, medium and low). We calculated the number of genes targeted by methylation by tallying all CpG methylated genes with copy number ≥1 that are present in at least one accession. These genes were categorized into 3 groups, namely, those with (i) high representation in most samples (appears in ≥90 samples, i.e. high group), (ii) medium representation across samples (appear in 40 to 90 samples, medium group), and (iii) low representation across samples (appear in less than 40 samples, low group). All genes in these groups were those targeted by CpG methylation. The genes in each group were collated as gene sets and analysed for the enrichment of significant molecular functions and corresponding over-represented GO terms. This analysis aids assessing any differences in the enrichment of gene sets from the groups, thereby enabling inference into the gene methylation profiles within each group. This also shades light into what enriched molecular functions can be associated with any phenotypic differences as a result of the underlying methylation profiles of targeted genes within each group.

Data filtering and inference: association between methylation and gene families. To investigate the association of methylation with gene families we extracted family clusters with at least 2 members from bread wheat. Wheat gene families were inferred using the OrthoFinder software[47]. We used the default parameters and recommendations given in the OrthoFinder manual. To improve the taxonomic resolution of the resulting gene families we included the comprehensive set of plant proteomes from Phytozome version 11[48] and the recently published barley gene catalogue[49]. Protein sequences of the clustered species were additionally screened for domain architectures with HMMER3 (PMID: 20180275) against the PFAM domain database (version 30) using the cut_ga option[50]. The resulting domain matches were filtered using the multi-objective optimization approach implemented in DAMA[51]. As protein catalogues from genome-wide predictions contain sequences derived from transposons and gene-fusion artefacts, the top orthogroups with the most members frequently are comprised of a mixture of gene families. To eliminate these from our analyses we have manually inspected the PFAM domain profiles of the clusters and finally excluded orthogroups with more than

40 distinct PFAM domains. The resulting set of 12,323 orthogroups was used as bona fide gene (sub) families comprising a total of 164,756 loci.

In all samples, gene families without any genes targeted by methylation were excluded from further analysis. There was a large variation in the size of targeted gene families and the number of genes within each gene family. Genes from targeted gene families (excluding larger-sized families, ≥40) were included in the analysis. The number of filtered genes was scaled by the size of the corresponding gene families since variations in the size of gene families might influence the results. This results in a proportional representation for targeted genes within each gene family. The use of proportions evens out any bias in the representation of targeted genes resulting from the larger-sized gene families. The heatmap.2 function (gplots R package) was used to generate dendrograms. A distance matrix was first generated using the *dist* function and then passed to the *hclust* function for hierarchical clustering. In all samples, gene families with an average of ≥25% representation of genes targeted by methylation were considered for GSEA using a targeted and non-targeted approach.

Generation of RNA-seq data for 12 samples for differential gene expression analysis.

Three seedlings were examined for all 12 lines from the A. E. Watkins bread wheat landrace collection (Supplementary table 22). Total RNA was extracted from the areal tissue of these 14-day-old wheat seedlings grown at a constant 24°C under long days using Qiagen RNeasy plant mini kits. Library preparation and RNA-seq was performed by the Earlham Institute platforms & pipelines using the Hiseq4000. Raw sequencing reads were trimmed for adapter sequence and also for regions where the average quality per base dropped below 15 (Trimmomatic version 0.32)[52]. After trimming, reads below 40bp in length were eliminated from the dataset. Trimmed reads for each sample were individually aligned to the Chinese Spring wheat reference genome using the splice-aware aligner HISAT2, which aligns RNA-seq reads to a reference while also identifying splice junctions[53]. Uniquely mapped reads were selected and duplicate reads filtered out to yield a "final mapped reads set" per sample. The program StringTie was implemented to assemble transcripts, guided by the read alignments to the reference genomes, and to estimate their abundances for each sample. Transcript assemblies or gene structure annotations could then be collated across the samples to form an analysis specific gene annotation summary i.e. a comprehensive list of all genes showing expression in at least one sample in the study. StringTie was then used to calculate gene and transcript abundances for each

sample across the analysis specific annotated genes. Finally, Ballgown allowed visualization of results and identification of differential expression between samples[53].

Ionomics. 12 plants for each Watkins accession were grown in groups of 4, and these were pooled (to give 3 replicate sets of plants, each replicate originating from one 'cigar roll'). All plants were grown on a standard nutrient solution[54]. For the three replicates of each Watkins accession, elemental analysis was performed on an ICP-MS (inductively coupled plasma mass spectrometry) and normalized concentrations of the samples were obtained as per the methods from Hosmani *et al.*[55]. Twenty elements (Li, B, Na, Mg, P, S, K, Ca, Mn, Fe, Co, Ni, Cu, Zn, As, Se, Rb, Sr, Mo, Cd) were monitored, of which Na and Zn were used here.

Transposon analysis. For each Watkins accession the cumulative coverage from the alignment of off-target reads to the TREP database was normalized to 50,000,000bp to match Chinese Spring most closely. Chinese Spring was also normalized to 50,000,000bp. For each transposon type, the base-space alignment coverage for Chinese Spring was subtracted from the corresponding Watkins accession value to yield a comparative value i.e. negative meaning the transposon showed higher coverage in Chinese Spring and positive meaning the Watkins accession showed higher coverage. These values were used to construct figure 4a, b and c.

Availability of supporting data

All sequencing datasets plus are available (study PRJEB23320) from the European Nucleotide archive (https://www.ebi.ac.uk/ena/submit/sra/#home). Our 12Mb capture design is also available on request.

Competing interests

The author(s) declare that they have no competing interests.

Authors' contributions /Acknowledgements

We thank Simon Orford who provided the Watkins seed (BBSRC funded ISP WISP). DNA sequence was generated by The University of Liverpool Centre for Genomic Research (United Kingdom). The

enrichment and Illumina sequencing library preparation was performed by LO with support from JK. SNP calling was performed by RJ. The RNA-SEQ work was performed by RRP. JO performed the gene family and gene-ontology analyses with support from MS and KM. The methylation analysis, genotype analysis, manuscript preparation, plant growth and DNA/RNA extraction was performed by LG. The project was designed, planned and conducted by LG and AH. The paper was written by LG and AH with assistance from NH and MB. All authors read and approved the final manuscript. We thank Anita Lucaci and Charlotte Nelson for their assistance with sequencing and library preparation respectively. Sadly, John Danku who performed the ICP-MS analysis for this study died before the data was submitted for publication

Funding

This project was supported by the BBSRC via an ERA-CAPS grant BB/N005104/1, BB/N005155/1 (L.G, A.H, MB), a BBSRC/DBT grant BB/L011786/1 (L.O.), IWYP project grant BB/N020871/1 (R.J) and BBSRC Design Future Wheat BB/P016855/1 (A.H, M.H).

Ethics Approval

Ethics approval was not needed for this study

References

1. Springer, N. M. and Schmitz, R, J. Exploiting induced and natural epigenetic variation for crop improvement. *Nature reviews genetics*, 18; 563-575 (2017)
2. Johannes, F. *et al.* Assessing the Impact of Transgenerational Epigenetic Variation on Complex Traits. *PLoS Genet* **5,** e1000530 (2009).
3. Hofmeister, B. T., Lee, K., Rohr, N. A., Hall, D. W. & Schmitz, R. J. Stable inheritance of DNA methylation allows creation of epigenotype maps and the study of epiallele inheritance patterns in the absence of genetic variation. *Genome Biology* **18,** 155 (2017).
4. Regulski, M. *et al.* The maize methylome influences mRNA splice sites and reveals widespread paramutation-like switches guided by small RNA. *Genome Research* **23,** 1651–1662 (2013).

5. Song, Q., Zhang, T., Stelly, D. M. & Chen, Z. J. Epigenomic and functional analyses reveal roles of epialleles in the loss of photoperiod sensitivity during domestication of allotetraploid cottons. *Genome Biology* **18,** 99 (2017).
6. Wang, C. *et al.* A transposon-directed epigenetic change in ZmCCTunderlies quantitative resistance to Gibberellastalk rot in maize. *New Phytologist* **215,** 1503–1515 (2017).
7. Kashkush, K., Feldman, M. & Levy, A. A. Transcriptional activation of retrotransposons alters the expression of adjacent genes in wheat. *Nature Genetics* **33,** 102–106 (2002).
8. Ong-Abdullah, M. *et al.* Loss of Karma transposon methylation underlies the mantled somaclonal variant of oil palm. *Nature* (2015). doi:10.1038/nature15365
9. Kawakatsu, T. *et al.* Epigenomic Diversity in a Global Collection of Arabidopsis thaliana Accessions. *Cell* **166,** 492–505 (2016).
10. Dubin *et al*. DNA methylation in Arabidopsis has a genetic basis and shows evidence of local adaptation. *eLife*, 1–23 (2015).
11. Kim, M. Y. & Zilberman, D. DNA methylation as a system of plantgenomic immunity. *Trends in Plant Science* 1–7 (2014). doi:10.1016/j.tplants.2014.01.014
12. Marcussen, T. *et al.* Ancient hybridizations among the ancestral genomes of bread wheat. *Science* **345,** 1250092 (2014)
13. Song, Q. & Chen, Z. J. Epigenetic and developmental regulation in plant polyploids. *Current Opinion in Plant Biology* **24,** 101–109 (2015).
14. Gardiner, L.-J. *et al.* A genome-wide survey of DNA methylation in hexaploid wheat. *Genome Biology* 1–15 (2015). doi:10.1186/s13059-015-0838-3
15. Wingen, L. U. *et al.* Establishing the A. E. Watkins landrace cultivar collection as a resource for systematic gene discovery in bread wheat, *Theor Appl Genet*, 127(8): 1831-42 (2014)
16. Olohan L*, Gardiner L*, Lucaci A, Kenny J and Hall A. A modified sequence capture approach allowing standard and methylation analyses of the same enriched genomic DNA sample. bioRxiv 209585; doi: https://doi.org/10.1101/209585 (2017)
17. Darst, R. P., Pardo, C. E., Ai, L., Brown, K. D. & Kladde, M. P. *Bisulfite Sequencing of DNA.* (John Wiley & Sons, Inc., 2001). doi:10.1002/0471142727.mb0709s91

18. Clavijo, B. J. *et al.* An improved assembly and annotation of the allohexaploid wheat genome identifies complete families of agronomic genes and provides genomic evidence for chromosomal translocations, *Genome Research*, 27(5):885-896 (2017)

19. Winfield, M. O. et al. High density genotyping of the A.E. Watkins Collection of hexaploid landraces identifies a large molecular diversity compared to elite bread wheat, Plant Biotechnology Journal, doi: 10.1111/pbi.12757 (2017)

20. Li, X. *et al.* Single-base resolution maps of cultivated and wild rice methylomes and regulatory roles of DNA methylation in plant gene expression. *BMC Genomics* **13,** 300 (2012).

21. Duncan, B. K and Miller, J. H. Mutagenic deamination of cytosine residues in DNA, *Nature*, **287:** 560-561 (1980)

22. Ossowski, S. *et al.* The rate and molecular spectrum of spontaneous mutations in Arabidopsis thaliana. *Science*, 327(5961):92-4 (2010)

23. Eichten, S. R., Stuart, T., Srivastava, A., Lister, R. and Borevitz, J. O. DNA methylation profiles of diverse Brachypodium distachyon align with underlying genetic diversity. *Genome Res.* **26(11):** 1520-1531 (2016)

24. Bouyer *et al.* DNA methylation dynamics during early plant life. *Genome Biology*, 18:179 (2017)

25. Yang, X., Han, H., Carvalho, D., Lay, F. D., Jones, P. and Liang, G. Gene body methylation can alter gene expression and is a therapeutic target in cancer, *Cancer Cell*, 26(4);577-590 (2014)

26. Brenet, F. *et al.* DNA methylation of the first exonis tightly linked to transcriptional silencing, *PLOSone*, 6(1);e14524 (2011).

27. Maussion, G. *et al.* Functional DNA methylation in a transcript specific 3'UTR region of TrkB associates with suicide. *Epigenetics*, 9(8):1061-70 (2014)

28. Apse, M.P., Aharon, G.S., Snedden, W.A. and Blumwald, E. Salt tolerance conferred by overexpression of a vacuolar Na+/H+ antiport in Arabidopsis. *Science*, 285(5431): 1256-8 (1999)

29. Szabolcs, I. Salt-affected soils in Europe. *The Hague, Martinus Nihoff*. 63p (1974)

30. Garcia, J. S., Souza, G, Eberlin, M. and Arruda, Z. Evaluation of metal-ion stress in sunflower (*Helianthus annus L.*) leaves through proteomic changes. *Metallomics*, 1:107-113 (2009)

31. Farinas, B. and Mas, P. Functional implication of the MYB transcription factor RVE8/LCL5 in the circadian control of histone acetylation, *Plant Journal*, 66;318-329 (2011)

32. Brenchley, R. *et al.* Analysis of the bread wheat genome using whole-genome shotgun sequencing. *Nature* **491,** 705–710 (2012).

33. Wicker, T., Matthews, D. E. and Keller, B. TREP: a database for Triticeae repetitive elements. *Trends Plant Sci.*, **7**, 561-562. (2002).

34. Lee, S. I. and Kim, N. S. transposable elements and genome size variations in plants. *Genomics Inform.*, 12(3):87-97 (2014)

35. Li, H. & Durbin, R. Fast and accurate short read alignment with Burrows-Wheeler transform. *Bioinformatics* **25,** 1754–1760 (2009).

36. Li, H. *et al.* The Sequence Alignment/Map format and SAMtools. *Bioinformatics* **25,** 2078–2079 (2009).

37. McKenna, A. *et al.* The Genome Analysis Toolkit: A MapReduce framework for analyzing next-generation DNA sequencing data. *Genome Res* **20,** 1297–1303 (2010)

38. Krueger, F. & Andrews, S. R. Bismark: a flexible aligner and methylation caller for Bisulfite-Seq applications. *bioinformatics.oxfordjournals.org* (2011)

39. Kurtz, S. *et al.* Versatile and open software for comparing large genomes. *Genome Biol.* **5(2):** R12 (2004)

40. Lister, R. *et al.* Highly integrated single-base resolution maps of the epigenome in Arabidopsis. *Cell* **133,** 523–536 (2008).

41. Fojtová, M., Kovařík, A. & Matyášek, R. Cytosine methylation of plastid genome in higher plants. Fact or artefact? *Plant Sci* **160,** 585–593 (2001).

42. Akalin, A. *et al.* methylKit: a comprehensive R package for the analysis of genome-wide DNA methylation profiles. *Genome Biol* **13,** R87 (2012)

43. Gardiner, L., Bansept-Basler, P., Olohan, L., Joynson, R., Brenchley, R., Hall, N., O'Sullivan, D. M. and Hall, A. Mapping-by-sequencing in complex polyploid genomes using genic

sequence capture: a case study to map yellow rust resistance in hexaploid wheat. *The Plant Journal*, **87 (4),** 403-419 (2016)

44. Chapman, J. A. *et al.* A whole-genome shotgun approach for assembling and anchoring the hexaploid bread wheat genome. *Genome Biol* **16,** 26 (2015).
45. Alexa, A., Rahnenführer, J. and Lengauer. T. Improved scoring of functional groups from gene expression data by decorrelating GO graph structure, *Bioinformatics*, 22(13): 1600-1607 (2006).
46. Wald, A. and Wolfowitz, J. On a test whether two samples are from the same population, Ann. Math Statist. 11, 147-162 (1940).
47. Emms, D. M. and Kelly, S. OrthoFinder: solving fundamental biases in whole genome comparisons dramatically improves orthogroup inference accuracy, Genome Biology, 16:157 (2015).
48. Goodstein, D. M. et al. Phytozome: a comparative platform for green plant genomics, *Nucleic Acids Res*. 40:D1178-86 (2012)
49. Mascher, M. et al. A Chromosome Conformation Capture Ordered Sequence of the Barley Genome, Nature 544 (7651), 427-433 (2017)
50. Finn, R. D. et al. The Pfam protein families database: towards a more sustainable future. Nucleic Acids Res, 44 (D1): D279-D285 (2016)
51. Bernardes, J. S., Vieira, F. R. J., Zaverucha, G., Carbone, A. A multi-objective optimization approach accurately resolves protein domain architectures, Bioinformatics, 32 (3): 345-353 (2016)
52. Bolger, A. M., Lohse, M. and Usadel, B. Trimmomatic: a flexible trimmer for illumina sequence data, *Bioinformatics*, **30(15):** 2114-2120 (2014)
53. Pertea, M., Kim, D., Pertea, G., Leek, J. and Salzberg, S. Transcript-level expression analysis of RNA-seq experiments with HISAT, StringTie, and Ballgown, *Nature Protocols*, **11(9):** 1650-1667 (2016)
54. Bai, C., Liang, Y. And Hawkesford, M. Identification of QTLs associated with seedling root traits and their correlation with plant height in wheat, *Journal of Experimental Botany*, 64(6): 1745-1753 (2013)
55. Hosmani P.S., *et al.* Dirigent domain-containing protein is part of the machinery required for

formation of the lignin-based Casparian strip in the root. *Proc Natl Acad Sci USA.* 27;110(35):14498-503 (2013)

Additional files

Additional file 1

Supplementary data file includes (PDF); figures 1-11, table 1-30

Additional file 2

Supplementary data file includes supplementary notes 1-12

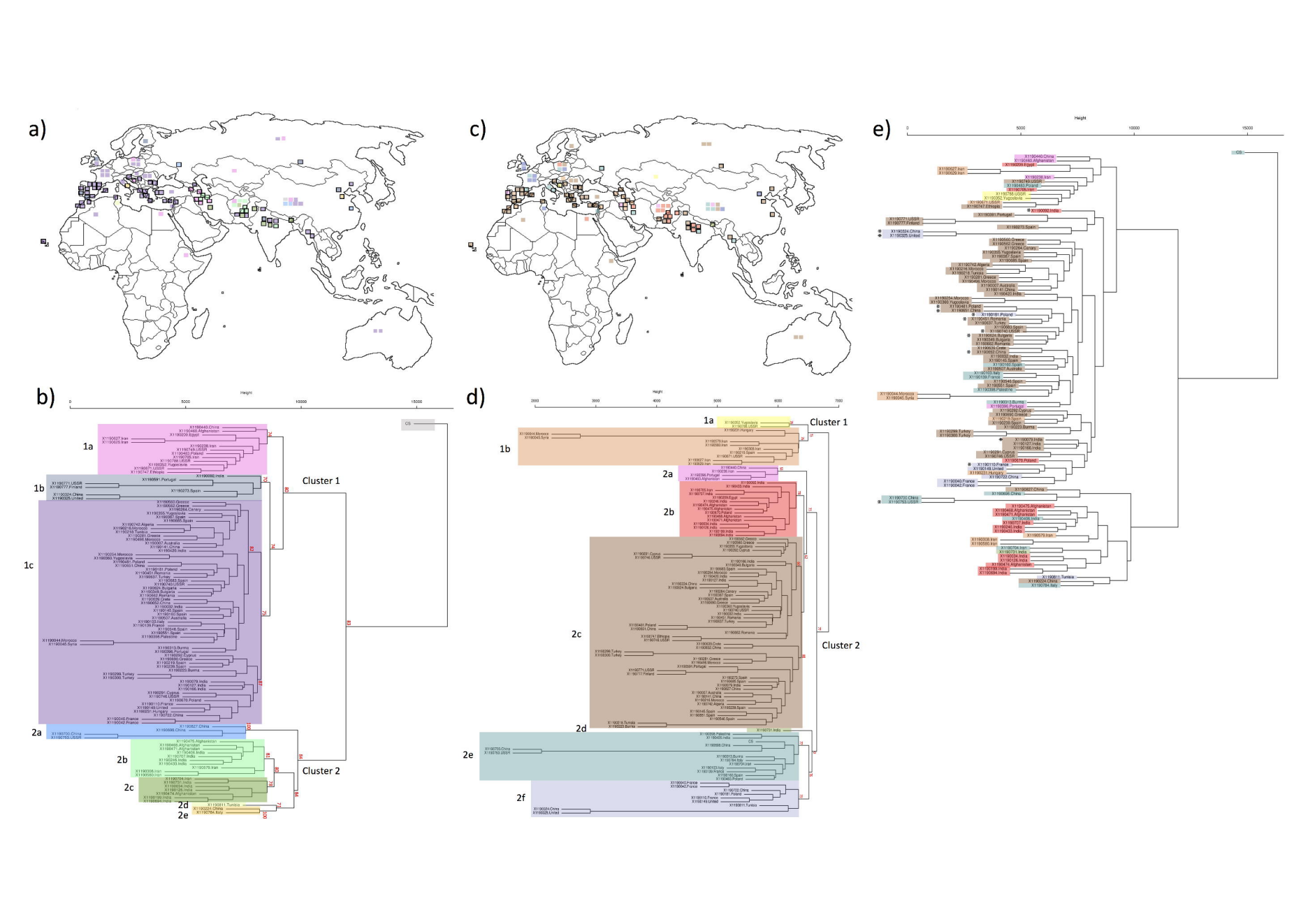
a)
b)
c)
d)
e)
Height
Cluster 1
Cluster 2
1a
1b
1c
2a
2b
2c
2d
2e
2f

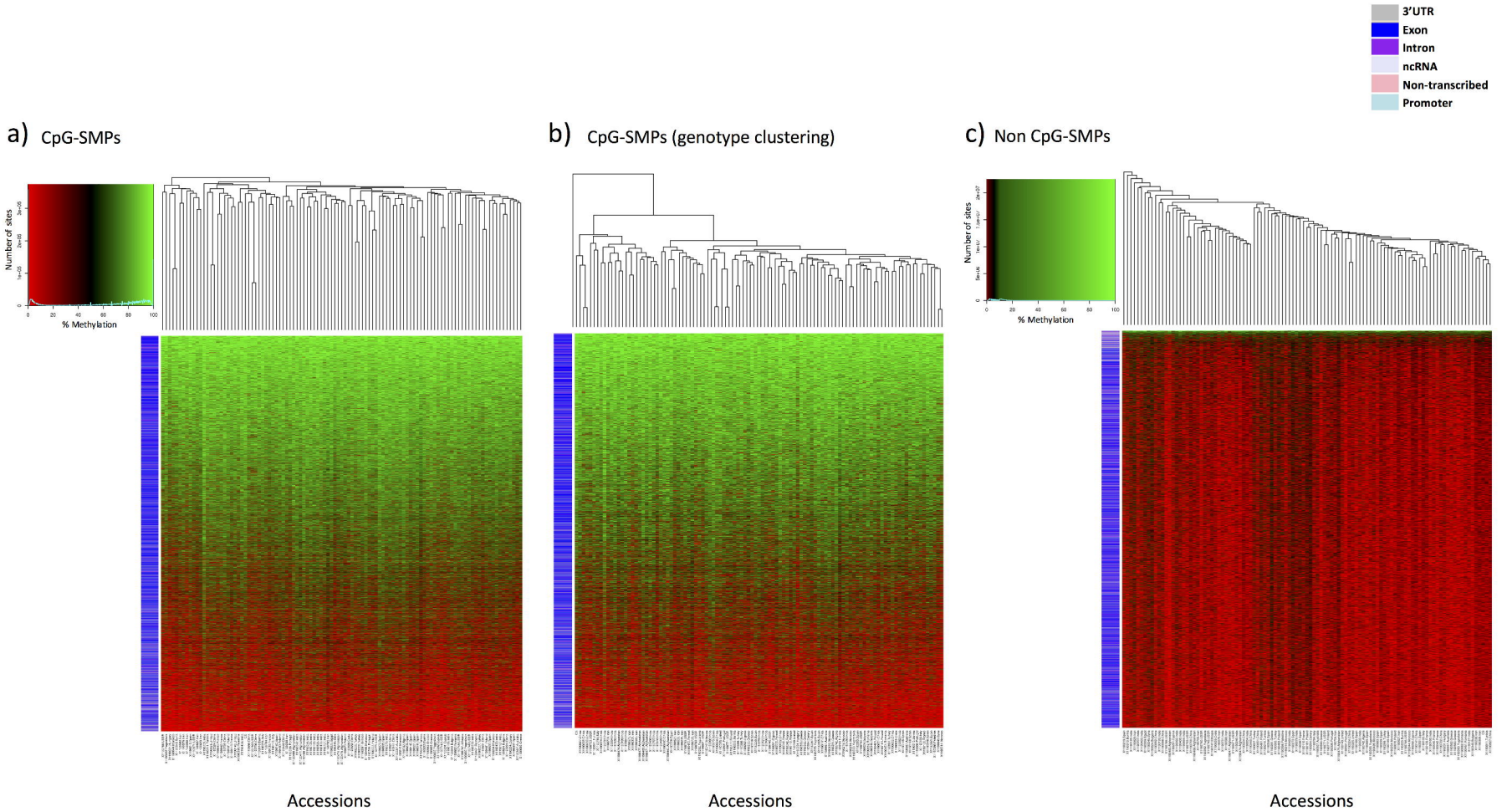
3'UTR
Exon
Intron
ncRNA
Non-transcribed
Promoter
a) CpG-SMPs
b) CpG-SMPs (genotype clustering)
c) Non CpG-SMPs
Number of sites
% Methylation
Accessions
Accessions
Accessions

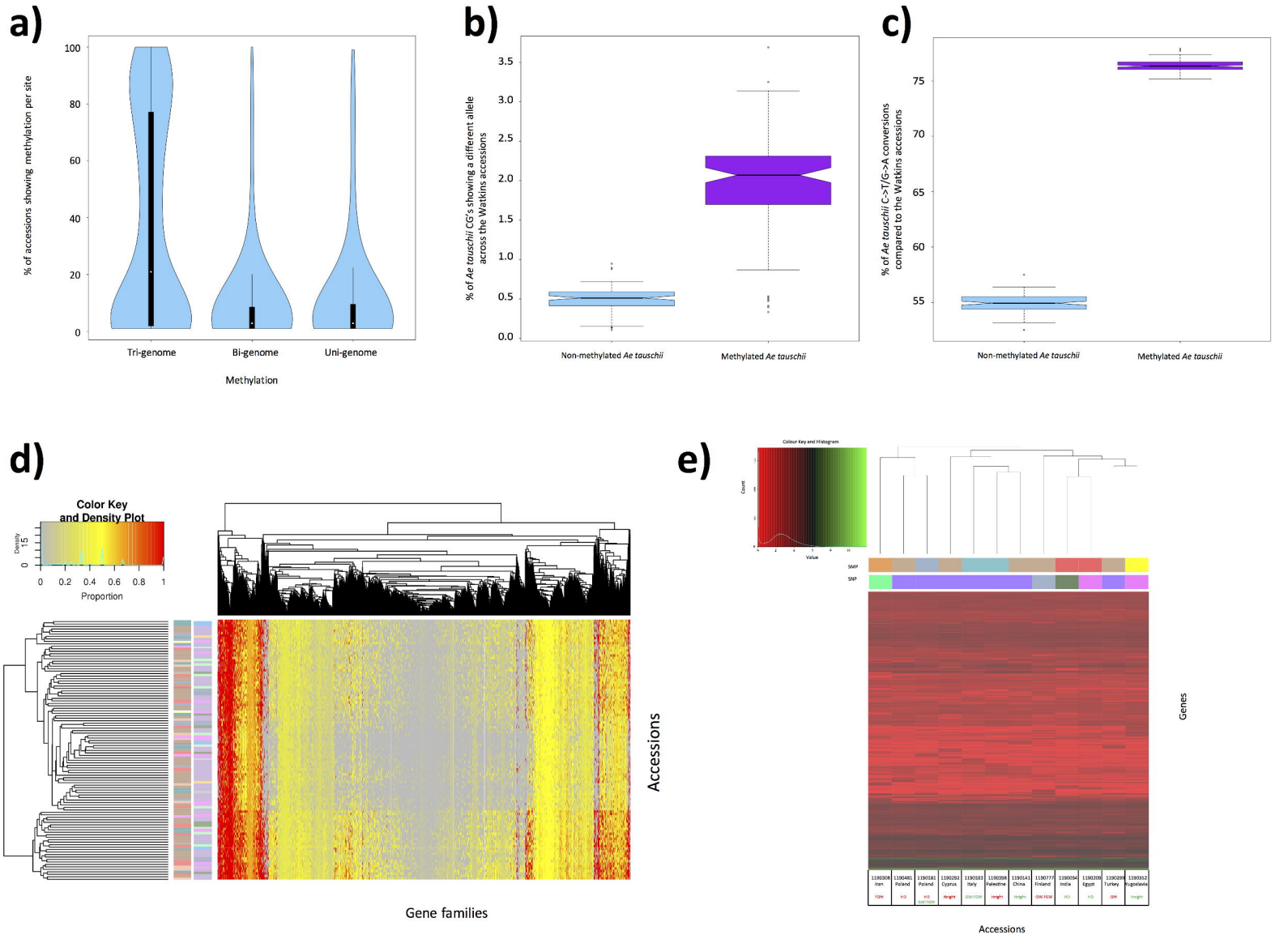
a)
% of accessions showing methylation per site
100
80
60
40
20
0
Tri-genome
Bi-genome
Uni-genome
Methylation
b)
% of Ae tauschii CG's showing a different allele across the Watkins accessions
3.5
3.0
2.5
2.0
1.5
1.0
0.5
0.0
Non-methylated Ae tauschii
Methylated Ae tauschii
c)
% of Ae tauschii C->T/G->A conversions compared to the Watkins accessions
75
70
65
60
55
Non-methylated Ae tauschii
Methylated Ae tauschii
d)
Color Key and Density Plot
Density
15
0
0
0.2
0.4
0.6
0.8
1
Proportion
Accessions
Gene families
e)
Colour Key and Histogram
Count
Value
SMP
SNP
Genes
Accessions

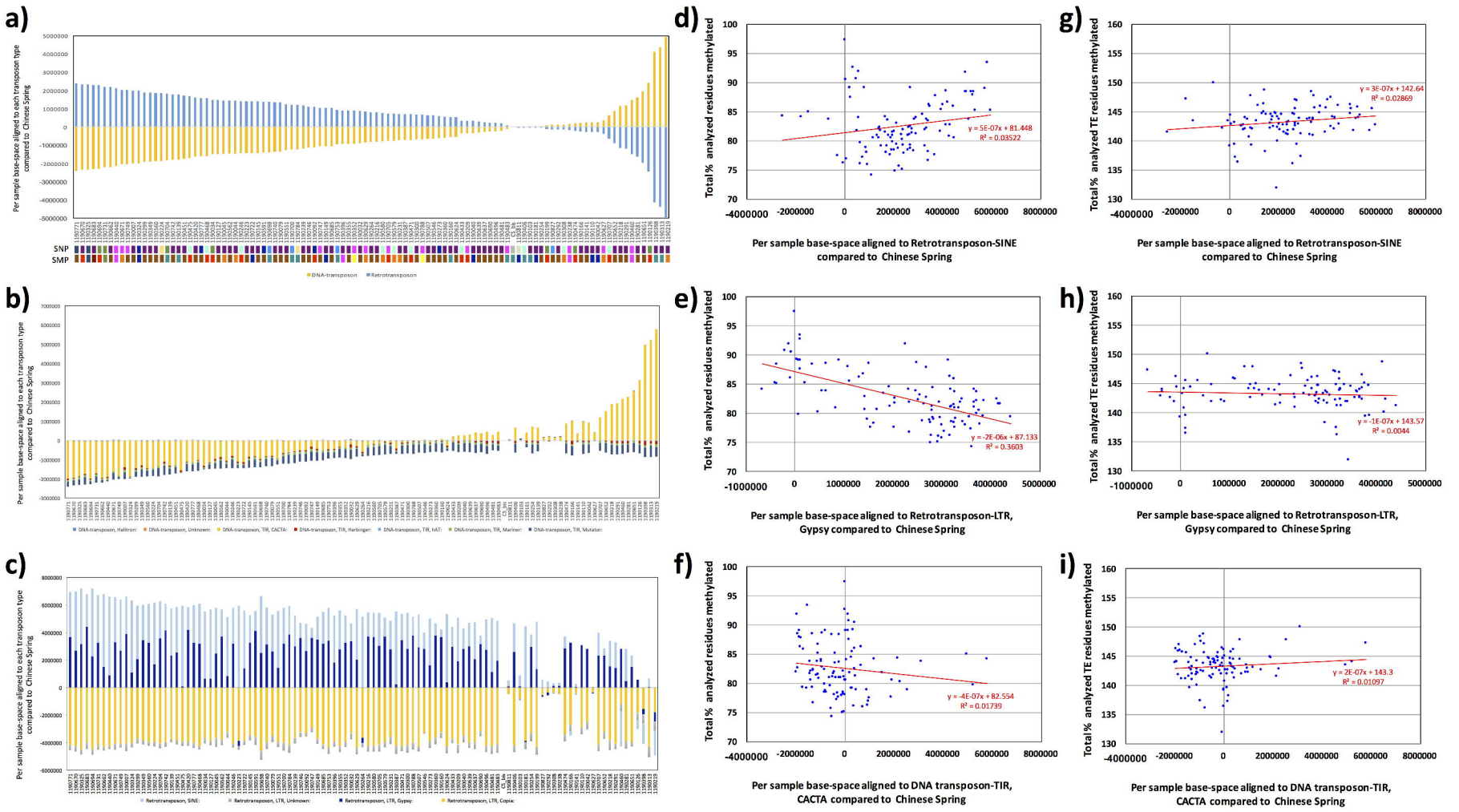
a)
b)
c)
d)
e)
f)
g)
h)
i)
Per sample base-space aligned to each transposon type compared to Chinese Spring
SNP
SMP
DNA-transposon
Retrotransposon
DNA-transposon, Helitron:
DNA-transposon, Unknown:
DNA-transposon, TIR, CACTA:
DNA-transposon, TIR, Harbinger:
DNA-transposon, TIR, hAT:
DNA-transposon, TIR, Mariner:
DNA-transposon, TIR, Mutator:
Retrotransposon, SINE:
Retrotransposon, LTR, Unknown:
Retrotransposon, LTR, Gypsy:
Retrotransposon, LTR, Copia:
Total% analyzed residues methylated
Total% analyzed TE residues methylated
y = 5E-07x + 81.448
R² = 0.03522
y = 3E-07x + 142.64
R² = 0.02869
Per sample base-space aligned to Retrotransposon-SINE compared to Chinese Spring
y = -2E-06x + 87.133
R² = 0.3603
y = -1E-07x + 143.57
R² = 0.0044
Per sample base-space aligned to Retrotransposon-LTR, Gypsy compared to Chinese Spring
y = -4E-07x + 82.554
R² = 0.01739
y = 2E-07x + 143.3
R² = 0.01097
Per sample base-space aligned to DNA transposon-TIR, CACTA compared to Chinese Spring